

AERODYNAMIC SHAPE OPTIMIZATION USING THE ADJOINT METHOD

Ernani V. Volpe, ernvolpe@usp.br
Department of Mechanical Engineering, University of Sao Paulo Av. Prof. Mello Moraes, 2231, CEP 05508-900, Sao Paulo – SP, Brazil

Luis C. C. Santos, luis.castro@embraer.com.br
Carlos A. Constantino, carlos.constantino@embraer.com.br
EMBRAER – Sao Jose dos Campos, SP, Brazil

Abstract. *Over the last two decades, CFD has become an essential tool in the aerospace industry. It provides a very cost-effective means for one to analyze different configurations. More recently, the development of inverse design and optimization methods has opened up new possibilities. On combining those methods with CFD codes, one can specify elaborate design goals and search for configurations that meet them. Among these, the so–called adjoint method stands out as the most promising approach to the problem. For it dramatically reduces the costs of computing sensitivity gradients, it allows total flexibility with respect to the flow physics model, and serves both purposes, optimization and inverse design. The rationale behind the adjoint method is to consider the problem within the framework of control theory. The flow field represents a system that is governed by differential equations. A set of control parameters and a measure of merit are defined in accordance with the design goals. Then the idea is to find the extrema of that measure of merit with respect to the control parameters, when the flow governing equations are imposed as constraints to the variation problem. This paper explores the conceptual foundations of the method and discusses its application in the case of quasi–1D nozzle flow.*

Keywords:*adjoint method, integral approach, adjoint boundary conditions, realizable flow variations*

1. INTRODUCTION

A typical optimization problem involves some measure of merit and a set of input parameters one is able to control. Then, a crucial step in the process is to evaluate the sensitivity of that measure to parameter variations. In fluid dynamics applications, this usually involves evaluating how flow variables change in response to variations in boundary conditions and/or geometry. In effect, it amounts to computing the gradient of the flow variables with respect to input parameters.

The conventional approach to the problem is to perturb each parameter, one at a time, and evaluate the corresponding changes in flow variables. The gradient is then computed by finite differences. A major liability of this method is that it often involves running a full simulation of the flow field for each parameter perturbation. Clearly, as the number of parameters increases, the computational cost becomes prohibitive.

Control theory offers an attractive alternative to this procedure. On using its concepts, one can derive a set of adjoint differential equations. Their solution allows one to obtain gradient information much more efficiently, without having to resort to costly finite differencing methods. As a result, the overall cost of the design procedure is greatly reduced, thus rivaling inverse design methods.

Once the sensitivity gradient is obtained, one can make use of any gradient based optimization algorithm to tackle optimization and inverse design problems. Besides, the general character of the adjoint method and the cost reduction it provides may be used to advantage in the context of certain inverse problems in fluid dynamics. That is the case when there is interest in investigating the sensitivity of flow related quantities to variations in boundary conditions parameters.

2. STATEMENT OF THE PROBLEM

Owing to its simplicity, the classical problem of Euler flow through a variable cross–section nozzle is chosen as an appropriate vehicle to explore the method underlying concepts. In particular, for a slowly varying cross–sectional area, the flow can be conveniently modeled by the well–known quasi–1D Euler equations ([Hirsch, 1994a]),

$$\frac{\partial(S\mathbf{Q})}{\partial t} + \frac{\partial(S\mathbf{F})}{\partial x} = S'\mathbf{H} \tag{1}$$

where $S = S(x)$ is the nozzle cross–sectional area, and $S' = \mathrm{d}S/\mathrm{d}x$ represents its slope. The quantities $\mathbf{Q}$ and $\mathbf{F}$ represent the state variables and flux vector in conservative form, respectively, and the term $S'\mathbf{H}$ on the the RHS accounts

for the effects of area change on the balance equations

$$\mathbf{Q} \equiv \begin{pmatrix} \rho \\ \rho u \\ \rho e_t \end{pmatrix} \quad ; \quad \mathbf{F} \equiv \begin{pmatrix} \rho u \\ \rho u^2 + P \\ (\rho e_t + P)u \end{pmatrix} \quad ; \quad \mathbf{H} \equiv \begin{pmatrix} 0 \\ P \\ 0 \end{pmatrix} \tag{2}$$

The ideal gas relation for pressure and the total energy per unit of mass (e_t)[1] closes the set (1).

$$P = (\gamma - 1)\rho \left[e_t - \frac{u^2}{2} \right] \tag{3}$$

As an illustrative example of a measure of merit, we define the following functional

$$I = \int_0^l g(\mathbf{V}) \, \mathrm{d}x \tag{4}$$

where $g(\mathbf{V})$ represents a generic scalar function of the primitive state variables $\mathbf{V} = (\rho, u, P)^T$. The integral is taken over the whole length of the nozzle, l, and the objective is to find the geometry $S(x)$ that minimizes functional I. On computing the variation of (4), one must take into account the possible occurrence of a normal shock wave within the flow domain. Hence, it is convenient to split the integration into two parts, upstream and downstream of the shock location x_s [Giles and Pierce, 2001]. This leads to

$$\delta I = \int_0^{x_s^-} \frac{\partial g}{\partial V}^T \cdot \frac{\partial V}{\partial Q} \cdot \delta \mathbf{Q} \, \mathrm{d}x - \left[g(V) \right]_{x_s^-}^{x_s^+} \delta x_s + \int_{x_s^+}^l \frac{\partial g}{\partial V}^T \cdot \frac{\partial V}{\partial Q} \cdot \delta \mathbf{Q} \, \mathrm{d}x \tag{5}$$

where δx_s represents a shift in the shock wave location. The rationale behind eq. (5) is that any changes in the flow field, $\delta \mathbf{Q}$ and δx_s, are brought about by variations in a set of control parameters, which has yet to be defined.

On assuming that the nozzle geometry can be accurately represented as a function of x with a set of parameters a_k, $S(x; a_k)$, one could attempt to minimize I by adjusting that set. Then the a_k would represent the control parameters, and the most important piece of information would be the sensitivity gradient $\partial I / \partial a_k$, which should be computed on the basis of eq. (5). The problem with that approach lies in the flow solution dependence on those parameters, which is not usually known in closed form. As a result, an estimate of $\partial \mathbf{Q} / \partial a_k$ would require several solutions of the flow governing equations (1), one for each variation δa_k, taken separately. Clearly, as the number of control parameters grows, the cost of such computations is bound to become prohibitively high.

A common trait of all the simulations required to estimate $\partial \mathbf{Q} / \partial a_k$ is that, for each individual variation δa_k, there must correspond a realizable solution to the flow governing equations. Hence, if one could constrain the variations to the space of realizable solutions, *a priori*. Then, perhaps, one could eliminate the need for expensive computations of $\partial \mathbf{Q} / \partial a_k$ to estimate the sensitivity gradient.

The adjoint method opens up such a possibility. Originally proposed by [Jameson, 1988] for aerodynamic applications, it makes use of concepts from control theory to achieve that goal. In essence, it imposes the flow governing equations as constraints on the optimization problem and, on doing so, it precludes unrealizable solutions. For the application in hand, one is mostly interested in steady flow conditions. Therefore, the steady form of eq. (1) is imposed on (4) as a non–holonomic constraint, thus leading to the augmented functional [Giles and Pierce, 1998, Giles and Pierce, 2000, Giles and Pierce, 2001]

$$I = \int_0^l g(\mathbf{V}) \, \mathrm{d}x + \underbrace{\int_0^l \Psi^T . \left(\frac{\partial (S\mathbf{F})}{\partial x} - S'\mathbf{H} \right) \mathrm{d}x + \Psi_s^T . \left[S\mathbf{F} \right]_{x_s^-}^{x_s^+}}_{I_c} \tag{6}$$

The third term on the RHS of eq. (6) imposes the Rankine–Hugoniot (R–H) relations on the shock wave, vectors Ψ^T and Ψ_s^T are the corresponding Lagrange multipliers. The symbol I_c is used to denote the whole set of constraints, and its first variation yields [Volpe and Santos, 2007]

$$\begin{aligned} \delta I_c \;=\; & \left[\Psi^T(x_s^-) - \Psi_s^T \right] . \delta \left(S\mathbf{F} \right)_{x_s^-} - \left[\Psi^T(x_s^+) - \Psi_s^T \right] . \delta \left(S\mathbf{F} \right)_{x_s^+} + \Psi_s^T . \left[S'\mathbf{H} \right]_{x_s^-}^{x_s^+} \delta x_s + \left[\Psi^T . \delta (S\mathbf{F}) \right]_0^l \\ & - \int_0^{x_s^-} \left[\frac{\partial \Psi^T}{\partial x} . \delta (S\mathbf{F}) + \Psi^T . \delta (S'\mathbf{H}) \right] \mathrm{d}x - \int_{x_s^+}^l \left[\frac{\partial \Psi^T}{\partial x} . \delta (S\mathbf{F}) + \Psi^T . \delta (S'\mathbf{H}) \right] \mathrm{d}x \end{aligned} \tag{7}$$

[1] $e_t = (e_i + u^2/2)$, where e_i represents the thermodynamic specific internal energy

The first two terms on the RHS of eq. (7) involve differences between the R–H Lagrange multipliers, Ψ_s, and the Ψ, where the latter are evaluated in the shock location. According to [Giles and Pierce, 1998, Giles and Pierce, 2000, Giles and Pierce, 2001], these terms prompt the need for an internal boundary condition that should be imposed on the Ψ, in that location. Then, on making

$$\Psi(x_s^-) = \Psi_s = \Psi(x_s^+) \tag{8}$$

those two terms drop from eq. (7), and one imposes the continuity of the Lagrange multipliers through the shock wave. Then on substituting $\delta(S\mathbf{F})$ and $\delta(S'\mathbf{H})$ with their variations and collecting like terms, one gets [Volpe and Santos, 2007]

$$\begin{aligned}
\delta I_c &= \Psi_s^T.\left[S'\mathbf{H}\right]_{x_s^-}^{x_s^+}\delta x_s + \left[\delta\mathbf{Q}^T.S\mathbf{A}^T.\Psi\right]_0^l + \left[\delta S\mathbf{F}^T.\Psi\right]_0^l + \\
&- \int_0^{x_s^-}\left[\delta\mathbf{Q}^T.\left(S\mathbf{A}^T\frac{\partial\Psi}{\partial x} + S'\mathbf{B}^T.\Psi\right) + \delta S\mathbf{F}^T.\frac{\partial\Psi}{\partial x} + \delta S'\mathbf{H}^T.\Psi\right]\mathrm{d}x + \\
&- \int_{x_s^+}^{l}\left[\delta\mathbf{Q}^T.\left(S\mathbf{A}^T\frac{\partial\Psi}{\partial x} + S'\mathbf{B}^T.\Psi\right) + \delta S\mathbf{F}^T.\frac{\partial\Psi}{\partial x} + \delta S'\mathbf{H}^T.\Psi\right]\mathrm{d}x
\end{aligned} \tag{9}$$

Both flow solution and geometry variations are implicitly assumed to be caused by control parameter changes, but they are otherwise taken to be independent of each other. The symbols $\mathbf{A}$ and $\mathbf{B}$ represent the flux Jacobian matrix ($\mathbf{A} = \partial\mathbf{F}/\partial\mathbf{Q}$) and the RHS term Jacobian matrix ($\mathbf{B} = \partial\mathbf{H}/\partial\mathbf{Q}$), respectively. As with the flux vector $\mathbf{F}$, one can easily show that $\mathbf{H}$ is homogeneous of degree one with respect to $\mathbf{Q}$. Hence, the relation $\mathbf{H} = \mathbf{B}.\mathbf{Q}$ holds as an exact result.

As a result of the Ψ continuity and of the fact that physical variables only undergo finite jump discontinuities through a shock wave, one can perform the integrations over the whole length of the nozzle, from 0 to l, as opposed to splitting them in the shock location— with the understanding that the flow governing equations hold there in the sense of weak solutions, only. Hence, the only remaining term that is directly related to the R–H conditions is the one that multiplies the shock wave shift δx_s.

Finally, the variation of the augmented functional (6) is gotten on adding the two eqs. (5) and (9) up and collecting like terms,

$$\begin{aligned}
\delta I &= \underbrace{\left[\delta\mathbf{Q}^T.S\mathbf{A}^T.\Psi\right]_0^l}_{(a)} + \underbrace{\int_0^l \delta\mathbf{Q}^T.\left[\left(\frac{\partial V}{\partial Q}\right)^T.\frac{\partial g}{\partial V} - S\mathbf{A}^T.\frac{\partial\Psi}{\partial x} - S'\mathbf{B}^T.\Psi\right]\mathrm{d}x}_{(b)} + \\
&+ \underbrace{\left\{\Psi_s^T.\left[S'\mathbf{H}\right]_{x_s^-}^{x_s^+} - \left[g(V)\right]_{x_s^-}^{x_s^+}\right\}\delta x_s}_{(c)} + \underbrace{\left[\mathbf{F}^T.\Psi\,\delta S\right]_0^l}_{(d)} - \underbrace{\int_0^l\left[\mathbf{F}^T.\frac{\partial\Psi}{\partial x}\,\delta S + \mathbf{H}^T.\Psi\,\delta S'\right]\mathrm{d}x}_{(e)}
\end{aligned} \tag{10}$$

The resulting equation represents the variation of the measure of merit subject to the chosen constraints. That is, it should satisfy the Euler equations in steady form, as well as the R–H relations. A split into geometric and physical variations can be promptly recognized, since the terms (d) and (e) involve only the former, whereas (a), (b) and (c) involve only the latter.

The variation split can be used to advantage in eliminating the $\delta\mathbf{Q}$ from the above equation. In principle, one can make use of the expression within brackets in (b) as a means to solve for Ψ. That can be accomplished by requiring it to satisfy the pde

$$-S\mathbf{A}^T\frac{\partial\Psi}{\partial x} - S'\mathbf{B}^T.\Psi + \frac{\partial V}{\partial Q}^T\frac{\partial g}{\partial V} = 0 \tag{11}$$

on both sides of the shock wave, thereby suppressing the integral from eq. (10). Boundary conditions for this pde are gotten from term (a), along with the continuity condition (8). It will be shown below that these conditions can be derived in such a way as to ensure that the problem is well–posed and that term (a) contribution to the total variation is zero. The term (c) will also be shown to have no contribution to δI.

Under these circumstances, the total variation reduces to the sum of (d) and (e), both of which involve only area variations. In essence, then, on solving (11) for Ψ and substituting the result in the expression of δI, one is implicitly constraining that variation to the space of realizable solutions. As a result, one should be able to estimate the sensitivity gradient without having to resort to expensive computations of individual design parameter variations.

Equation (11) corresponds to the adjoint equation for the problem. However it can be cast in a more instructive form, which stresses its similarity to the flow governing equation (1). The importance of such similarity is twofold: not only does it indicate an approach to solving the adjoint equation; but, more importantly, it gives us guidance in deriving appropriate boundary conditions to impose on it.

3. THE ADJOINT EQUATION

The similarity between the adjoint pde (11) and the Euler equation (1) becomes apparent when one writes the latter in terms of the Jacobian matrix $\mathbf{A}$ and makes use of the identity $\mathbf{H} = \mathbf{B}.\mathbf{Q}$. On introducing these results into the steady form of (1) and comparing it to (11) one gets

$$-S\mathbf{A}^T\frac{\partial\Psi}{\partial x} - S'\mathbf{B}^T.\Psi = -\frac{\partial V}{\partial Q}^T\frac{\partial g}{\partial V} \equiv -\frac{\partial g}{\partial Q} \tag{12}$$

$$S\mathbf{A}\frac{\partial\mathbf{Q}}{\partial x} - S'\left(\mathbf{B}-\mathbf{A}\right).\mathbf{Q} = 0 \tag{13}$$

As can be seen, both equations share a similar structure. The only differences are in the sign of the flux term and the non–homogeneous term on the RHS of (12). The origin of the latter can be traced back to the variation of the objective functional in eq. (5). Whereas the terms on the LHS of eq. (12) all come from the variation of the governing equation (9) and bear no influence of the objective functional.

The apparent similarity between the two pdes opens up the possibility of using the same body of knowledge that has been developed for the Euler equation to tackle the adjoint equation. The hyperbolic character the Euler equation exhibits in the time–space domain is what ultimately determines flow boundary conditions. Given the structure of (12), the same feature could be shared by the adjoint equation if only one could postulate a time dependence for the variable Ψ similar to $\mathbf{Q}$. In principle, that could be accomplished by simply adding a time derivative to the LHS of (12). This step leads to the following pde

$$\frac{\partial(S\Psi)}{\partial t} - S\mathbf{A}^T\frac{\partial\Psi}{\partial x} - S'\mathbf{B}^T.\Psi = -\frac{\partial g}{\partial Q} \tag{14}$$

$$\frac{\partial(S\mathbf{Q})}{\partial t} + S\mathbf{A}\frac{\partial\mathbf{Q}}{\partial x} - S'\left(\mathbf{B}-\mathbf{A}\right).\mathbf{Q} = 0 \tag{15}$$

which is paired with the full Euler equation for comparison. In view of the relation between the two, the flow and the optimization are usually referred to as primal and dual problems, respectively ([Giles and Pierce, 1999]). For its role in the latter, Ψ is often referred to as the co–state vector in the literature. The same terminology shall be adopted henceforth.

Clearly, one is only interested in the steady solution to (14), which actually recovers eq. (12) as the time derivative vanishes. Equation (14) is just a model equation, but it does fulfill its role regarding the hyperbolic character. In its final form, the adjoint eq. (14) shares the same characteristics as the Euler eq. (15), but for a reversal of sign of the characteristic velocities. Quite different from the latter, though, the adjoint eq. is linear. For neither the flux Jacobian $\mathbf{A}$ nor the matrix $\mathbf{B}$ depend on Ψ.

An immediate consequence of the adjoint equation linearity is the fact that singularities can only travel along characteristics, and they must be borne by the Cauchy data ([Lax, 1973, Leveque, 2002]). Then, there is no reason for the Ψ to develop jump discontinuities anywhere in the solution domain, unless they are brought in by the boundary or initial conditions. That is the case of the sonic line singularity $(u-a) = 0$, which is reported in the literature ([Giles and Pierce, 1997]).

In a strict sense, the shock wave divides the flow field into two solution domains for the adjoint equation, and they are connected by the continuity condition (8). A numerical method, however, may handle that connection in either of two ways: by enforcing (8) explicitly at the shock location, as in a shock fitting approach; or, alternatively, by treating the shock as a discontinuity within the domain, in a fashion that is quite similar to the shock capturing methods of flow simulation. The second option is usually preferred over the first one because it should, in principle, involve a simpler implementation of the method.

In any case, the behavior of co–state variables Ψ through the shock wave can be analyzed with the aid of the adjoint equation (14) and of the term (c) in the total variation (10). That term imposes a condition on a control volume of infinitesimal thickness that encloses the shock wave, and it implies

$$\left(g^+ - g^-\right) = \Psi_s^T.\left[\left(S'\mathbf{H}\right)^+ - \left(S'\mathbf{H}\right)^-\right] \tag{16}$$

where the symbols $(\ )^-$ and $(\ )^+$ stand for conditions on the upstream and downstream sides of the shock wave, x_s^- and x_s^+ respectively. On making use of the Ψ continuity, the R–H conditions and the stationary form of the adjoint equation (14), one gets [Volpe and Santos, 2007]

$$\left(g^+ - g^-\right) = +\left.\frac{\partial g}{\partial Q}\right|_+^T\mathbf{Q}^+ - \left.\frac{\partial g}{\partial Q}\right|_-^T\mathbf{Q}^- - \left(\left.\frac{\partial\Psi}{\partial x}\right|_+^T - \left.\frac{\partial\Psi}{\partial x}\right|_-^T\right).\left(S\mathbf{F}\right)^+ \tag{17}$$

The above equation relates the co–state variables to the nature of the objective function $g(V)$: If this function is homogeneous of degree one with respect to $\mathbf{Q}$, then the Ψ first derivative must be continuous through the shock wave, which, in turn, implies that the co–state variables are continuous of class $\mathcal{C}^1$. If that is not the case, then the Ψ first derivative undergoes a jump discontinuity through the shock, the intensity of which is given by (17).

3.1 Boundary Conditions for the Adjoint Equation

As was discussed above, the steady solution to the adjoint equation (14) should allow one to eliminate the integral (b) from the the total variation δI (10). Boundary conditions for that equation can be derived from (a), which would then be the only remaining term in the variation that involves $\delta\mathbf{Q}$

$$\left[\delta\mathbf{Q}^T.S\mathbf{A}^T.\Psi\right]_0^l = \left(\delta\mathbf{Q}^T.S\mathbf{A}^T.\Psi\right)_l - \left(\delta\mathbf{Q}^T.S\mathbf{A}^T.\Psi\right)_0 \tag{18}$$

Besides being consistent with the pde (14), these boundary conditions should ideally eliminate the above terms from the total variation δI, thus suppressing its dependence on the state vector variation.

The terms in (18) involve both state and co–state vectors at the boundaries of the flow domain. The state vector variation is governed by flow boundary conditions, which impose relations among its components, δq_i. Boundary conditions for the ψ_i should follow the same reasoning, given the similarity between the pdes. Only the sign reversal of the characteristics leads to boundary conditions that are complementary to those of the primal problem. As will be shown below, it is this relation between primal and dual boundary conditions that ultimately enables one to eliminate all terms in (18) from δI.

The rationale behind the adjoint boundary conditions is best conveyed on replacing the terms $\mathbf{A}$ and $\delta\mathbf{Q}$ by their counterpart, $\mathbf{A}\delta\mathbf{Q} = \delta\mathbf{F}$. That leads to an alternative form for eq. (18)

$$\left[S\delta\mathbf{F}^T.\Psi\right]_0^l = \left(S\delta\mathbf{F}^T.\Psi\right)_l - \left(S\delta\mathbf{F}^T.\Psi\right)_0 \tag{19}$$

Both terms on the RHS of eq. (19) involve scalar products between the co–state variables Ψ and flux variations $\delta\mathbf{F}$ at the boundaries of the flow domain. The nullity of these products implies the Ψ should be orthogonal to all realizable flux variations $\delta\mathbf{F}$— the term *realizable*, here, means those that satisfy the flow governing equations. This way, the co–state variables may be thought of as *generalized constraint forces* that impose mass, momentum and energy conservation on all flux variations at the boundaries. Therein lies a possible interpretation of the Ψ and their boundary conditions.

Given the way the variational problem is constructed, the same interpretation of the co–state variables should actually hold throughout the flow domain, as opposed to just the boundaries. It suffices to recall that $\delta\mathbf{Q}$ (term b in eq.10) must be realizable, but it is otherwise arbitrary. Hence the only way to make that integral null is to take Ψ as the solution to the adjoint equation. Within this framework, the rationale behind the method is akin to minimizing the virtual work of the generalized constraint forces Ψ, thereby ensuring that the system trajectory in state space is fully realizable. Although these ideas do not have any direct bearing on the algebra, they can guide us through the derivation that follows.

As was mentioned above, the flux Jacobian of the adjoint equation (14) is the same as that of the Euler equation, except for the transposition and sign reversal. Therefore, it has the same characteristic velocities, but with opposite signs: $-u, -(u+c), -(u-c)$. Figure 1 illustrates the situation in an arbitrary quasi–1D nozzle. It depicts both primal dual characteristics under different flow conditions.

Boundary conditions for supersonic flow at an entrance impose constant values on all state vector components q_i. That, in turn, implies that all of their variations are zero: $\delta q_i = 0$. Since the adjoint characteristics run in the opposite direction, the co–state variables should not be imposed any boundary conditions there. As a result, the corresponding ψ_i are free, but the nullity of $\delta\mathbf{Q}$ ensures that $\left(\delta\mathbf{Q}^T.S\mathbf{A}^T.\Psi\right)_0 = 0$ at that boundary. To put it another way, $\delta\mathbf{Q} = 0 \;\Rightarrow\; \delta\mathbf{F} = 0$. Therefore, the orthogonality condition holds for any vector Ψ.

At a supersonic exit, no boundary conditions are imposed on $\mathbf{Q}$ and, thus, all variations δq_i are left unspecified. However, the reverse sign of the adjoint characteristics implies that all ψ_i must be imposed boundary conditions there. In principle, these could be picked so as to ensure that $\left(\delta\mathbf{Q}^T.S\mathbf{A}^T.\Psi\right)_l = 0$ at that boundary. That can be accomplished by simply imposing homogeneous boundary conditions on the co–state variables: $\psi_i = 0$. Here again, the unspecified δq_i imply that all $\delta\mathbf{F}$ are allowed, hence the need for imposing homogeneous boundary conditions on Ψ.

Boundary conditions for subsonic flow need more careful consideration. For in that case there are characteristics that run both ways, upstream and downstream, and flux variations at the boundaries are constrained. The idea is to evaluate the realizable $\delta\mathbf{F}$ in each case, and then to find out the Ψ that are orthogonal to these variations.

At a subsonic entrance, the boundary conditions impose the flow direction, along with constant values for the stagnation pressure P_o and temperature T_o, thereby implying that their variations are zero. Owing to the quasi–1D character of this particular application, only the latter two quantities are considered. On proceeding as was outlined above, one gets the following boundary condition [Volpe and Santos, 2007]

$$\psi_1 = \left[\frac{(\gamma-1)u^2}{2} - e_t\gamma\right]\psi_3 - u\psi_2 \tag{20}$$

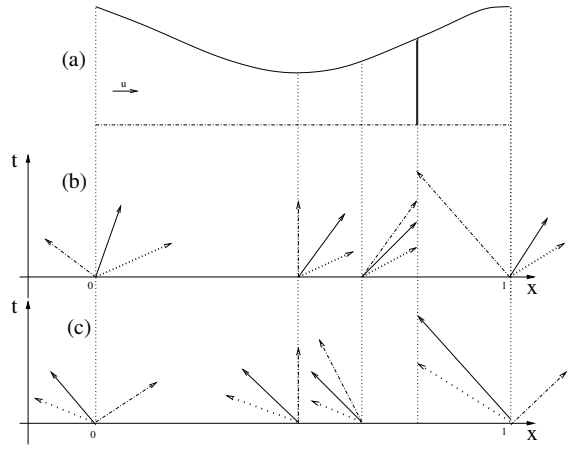

Figure 1. Quasi–1D nozzle flow. (a) Physical space, with sonic conditions at the throat and a normal shock wave in the divergent portion— represented by a double solid line. (b) Flow characteristics: solid line, u; dotted line, $(u+c)$; dash–dot line, $(u-c)$. (c) Adjoint characteristics: solid line, $-u$; dotted line, $-(u+c)$; dash–dot line, $-(u-c)$.

to be imposed on the ψ_i at a subsonic entrance. It is worth noting that, on imposing $\psi_1 = \psi_1(\psi_2, \psi_3)$, one is effectively constraining one degree of freedom (dof), which corresponds to the adjoint characteristic that runs into the flow domain. Two remaining dofs are preserved, and they correspond to the two characteristics that convey information from the domain to the entrance boundary, fig. 1.c.

Flow physics implies that the static pressure P, alone, be specified at a subsonic exit boundary. On following the same procedure as above, the corresponding adjoint boundary conditions are given by [Volpe and Santos, 2007]

$$\begin{cases} \psi_1 = \left[\gamma e_t - \frac{(\gamma-1)u^2}{2}\right]\psi_3 \\ \psi_2 = \left[\frac{(\gamma-2)u}{2} - \frac{\gamma e_t}{u}\right]\psi_3 \end{cases} \tag{21}$$

which should be imposed at a subsonic exit. Equations (21) constrain two dofs, which correspond to the two adjoint characteristics that run into the flow domain. One remaining dof is preserved, and it corresponds to the single characteristic that conveys information from the domain to the exit boundary.

4. INVERSE DESIGN APPLICATION

Given the general structure of the adjoint equation (14), the above results can be illustrated with a simple inverse design application. The measure of merit is defined as the mean square error of the actual pressure distribution P with respect to a target distribution P_D

$$I = \frac{1}{2}\int_0^l (P - P_D)^2 \, \mathrm{d}x \tag{22}$$

The integrand of functional (22) yields the following gradient with respect to the state variables $\mathbf{Q}$:

$$\frac{\partial g}{\partial Q} = (P - P_D)(\gamma - 1)\begin{pmatrix} \frac{u^2}{2} \\ -u \\ 1 \end{pmatrix} \tag{23}$$

This expression gives rise to the non–homogeneous term of the adjoint pde (14). Moreover, it can be shown that g is not a homogeneous function of degree one on $\mathbf{Q}$. According to eq. (17) it implies that the ψ_i derivatives should undergo jump discontinuities through a shock wave, and these should meet the relation

$$\left(\left.\frac{\partial \Psi}{\partial x}\right|_+^T - \left.\frac{\partial \Psi}{\partial x}\right|_-^T\right) \cdot (S\mathbf{F})^+ = \frac{1}{2}\left[P^2 - P_D^2\right]_-^+ \tag{24}$$

If the nozzle geometry can be cast in the generic form $S = S(x; a_k)$, for $k = 1, ..., n$, and Ψ satisfies (14). Then the

sensitivity gradient is obtained directly from eq. (10), terms (d) and (e),

$$\frac{\partial I}{\partial a_k} = \left[\mathbf{F}^T.\Psi\frac{\partial S}{\partial a_k}\right]_0^l - \int_0^l \left[\mathbf{F}^T.\frac{\partial \Psi}{\partial x}\frac{\partial S}{\partial a_k} + \mathbf{H}^T.\Psi\frac{\partial S'}{\partial a_k}\right] \mathrm{d}x \tag{25}$$

On picking a particular family of functions to represent $S(x;a_k)$, say polynomials, one is able to evaluate the derivatives $\partial S/\partial a_k$ in closed form.

In any case, the adjoint pde is solved on the basis of a steady converged solution to the Euler equations. So that all of its coefficients are known beforehand and remain constant throughout the adjoint solution process. The inverse design application comprises a sequence of: flow simulation for a given geometry, adjoint solution, gradient evaluation and gradient based optimization procedure. The last step leads to a new geometry and, thus, closes the cycle. The cycles are repeated until a local extremum of the measure of merit is reached, within a prescribed accuracy level.

A single piece of code was written to tackle the whole procedure. The Euler equations are integrated explicitly by a split–flux based algorithm with three alternative methods: Steger–Warming, Modified Steger–Warming and Roe. The adjoint pde is solved by means of the Beam and Warming three point backward implicit scheme, to which artificial dissipation was added ([Hirsch, 1994b, Pulliam, 1986]). The conjugate gradient algorithm was picked as the optimization method ([Vanderplaats, 1984]).

For the purpose of comparison, a program was dedicated to computing the sensitivity gradient by brute–force, over the same search path that had been pursued by the adjoint. To that end, each control parameter is perturbed separately about its original value in the baseline configuration. The gradient is evaluated by a central finite difference scheme to second order accuracy. Two perturbed flow simulations are needed for each parameter, in addition to the baseline solution.

For the sake of space, only one set of test results is shown below, with the aim of illustrating the adjoint boundary conditions. The target P_D is taken as the actual pressure distribution of a specific geometry, under given flow conditions. Although unusual in actual applications, the procedure ensures two essential features of the validation tests: not only is the target realizable, but its geometry is known beforehand. For simplicity, $S(x;a_k)$ is chosen as a second order polynomial with three control parameters. Accuracy levels have been set to: 10^{-5} for the flow and adjoint solutions. The Modified Steger–Warming method has been picked for all flow simulations.

The test concerns a converging–diverging nozzle under the following boundary conditions[2]: $P_o = 20.0$ and $T_o = 7.26$ at the entrance, and the static back pressure $P_b = 15.0$. Results were gotten in 50 inverse design cycles. Figure 2 presents geometry and pressure evolution, fig. 3 shows the first and last adjoint solutions and fig. 4, left, depicts the sensitivity gradient evolution.

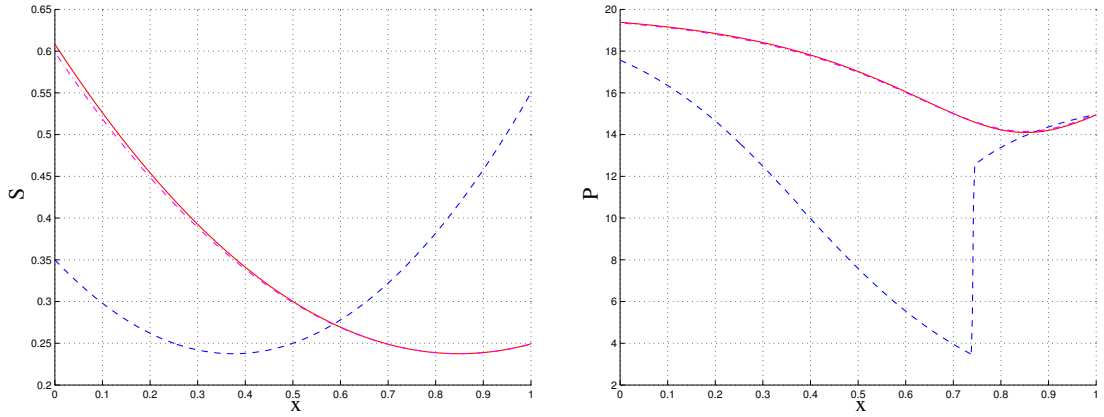

Figure 2. Transonic flow through a convergent–divergent nozzle. Left, geometry evolution. Right, pressure evolution. Dashed lines, original curves; solid lines, final results; dash–dot lines, target profiles.

The nozzle throat area has been constrained to a fixed value, so as to limit the maximum mass flow rate. The minimum area was imposed as an external constraint, by a relation among the control parameters. The procedure was designed so as not to interfere with the gradient computation, but to change the search direction, only. The target pressure distribution P_D has been set for subsonic isentropic flow, which is feasible within the active constraints.

As can be seen, the original pressure distribution has a shock wave in the nozzle divergent portion (fig. 2), which implies that the throat flow is choked. Indeed, the first adjoint solution (fig. 3, left) exhibits the characteristic singularity at the throat, as it has been reported in the literature ([Giles and Pierce, 1997, Giles and Pierce, 2001]) and was mentioned above.

[2]Dimensionless properties are scaled to a reference state

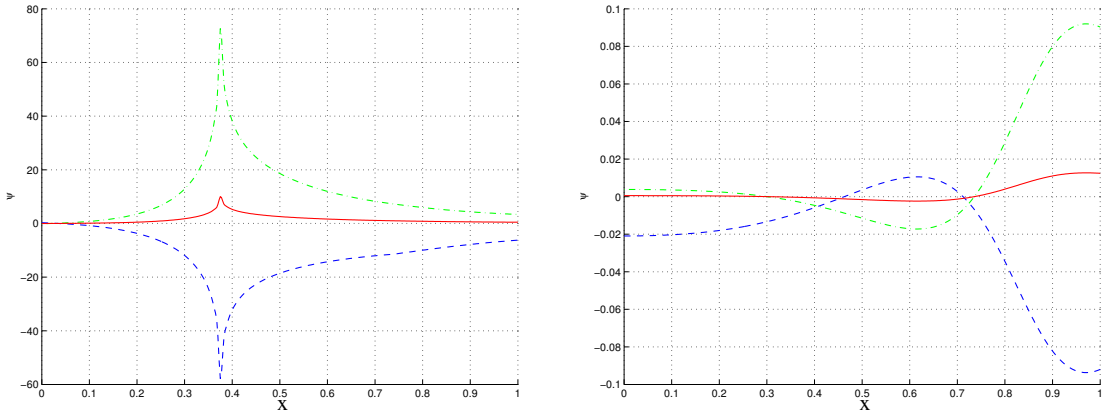

Figure 3. Transonic flow through a convergent–divergent nozzle. Adjoint equation solutions: left, first solution; right, last solution. Dash–dot lines, ψ_1; dashed lines ψ_2; solid lines ψ_3.

On the other hand, the Ψ does not seem to undergo any noticeable slope discontinuity at the shock location. The whole picture changes when one evaluates the terms in relation (24), which are plotted in fig. 4, right. There, one clearly sees that both the Ψ derivative (solid line) and the pressure square difference (dashed line) undergo finite jumps at the shock wave location, precisely. Furthermore, the jumps appear to have the same strength, within the accuracy of these estimates: the former is about 73.58, whereas the latter is about 74.43. It must be noted that the term $\partial\Psi/\partial x$ shows another discontinuity in fig. 4, right, but this one is a direct result of the Ψ singularity at the nozzle throat.

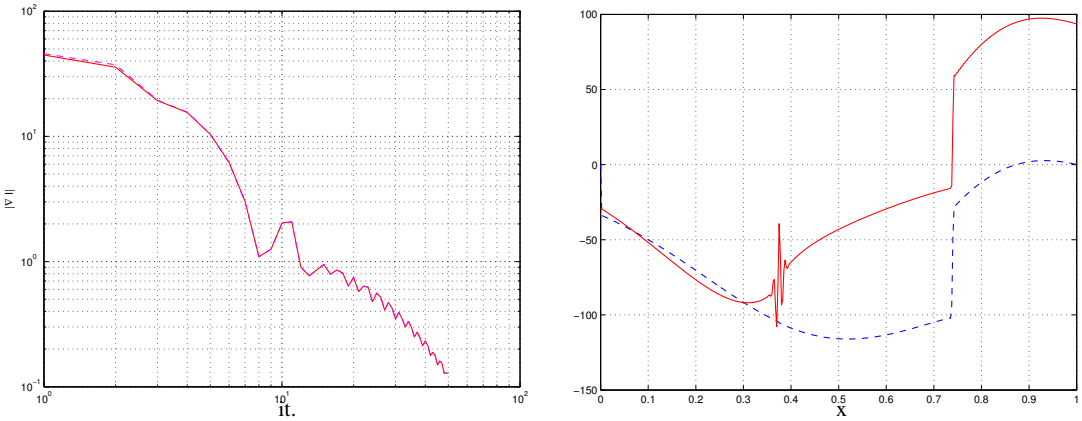

Figure 4. Transonic flow through a convergent–divergent nozzle. Left, gradient magnitude evolution: solid Line, adjoint method; dash–dot line, brute–force. Right, discontinuities in $\partial\Psi/\partial x$ at the first inverse design cycle. In reference to eq. (24): solid Line, $(\partial\Psi/\partial x)^T.(S\mathbf{F})$; dashed line, $g(\mathbf{V}) = (P^2 - P_D^2)/2$.

As the cycles progress and the solution approaches P_D, the flow becomes fully subsonic, the mass flow rate drops from its limiting value, the ψ_i become smooth functions (fig. 3, right) and their magnitude also drops off.

The sensitivity gradient evolution is shown in fig. 4, left. The gradient has also been estimated by brute–force, at the same points as the adjoint method. A comparison between the two reveals the error of the latter, with respect to the former method, reaches a peak of 4.5% in the first few cycles and then drops below 0.03%. Further tests seem to indicate a link between that behavior and the numerical error incurred by solving the adjoint characteristics at the domain boundaries.

4.1 A Linear Objective Functional

Still in regard to the adjoint variables behavior through the shock wave, it is instructive to consider an alternative measure of merit. Equation (17) shows that any objective functional, which is homogeneous of degree one with respect to the state variables $\mathbf{Q}$, should lead to smooth ψ_i of class $\mathcal{C}^1$. Such a functional would make for an illustrative comparison with the previous case of eq. (24) and fig. 4, right. Then, it should be interesting to pick the same pressure integral that

has been used by [Giles and Pierce, 2000, Giles and Pierce, 2001].

$$I = \int_0^l P \, \mathrm{d}x \tag{26}$$

For which the integrand yields the gradient

$$\frac{\partial g}{\partial Q} = (\gamma - 1) \begin{pmatrix} \frac{u^2}{2} \\ -u \\ 1 \end{pmatrix} \tag{27}$$

As before, the expression corresponds to the non–homogeneous term of the adjoint pde (14). However, in this case it can be seen that $g(\mathbf{Q})$ is an homogeneous function of degree one and, as a result, the ψ_i derivatives should undergo no jumps through the shock wave. That is, they should meet the condition

$$\left(\frac{\partial \Psi}{\partial x}\bigg|_+^T - \frac{\partial \Psi}{\partial x}\bigg|_-^T \right) . (S\mathbf{F})^+ = 0 \tag{28}$$

which implies continuity, given that the flux $(S\mathbf{F})$ through the shock wave is obviously non–zero.

A test was set up where the adjoint solution is computed for the objective functional (26), in the same original geometry and under the same conditions as the converging–diverging nozzle above. The results thus obtained are presented in fig. 5, and they should be compared to those of the first cycle in the previous case.

On the left, fig. 5 presents the solution for ψ_i, which should be compared to fig. 3–left. On the right it depicts the term $(\partial\Psi/\partial x)^T.(S\mathbf{F})$ and the pressure distribution— the latter picture should be compared to fig. 4, right.

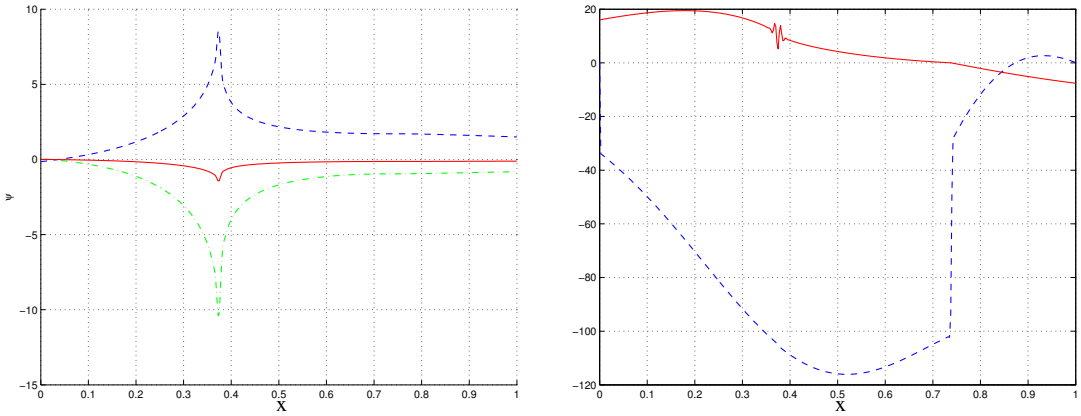

Figure 5. Transonic flow through a convergent–divergent nozzle. Left, adjoint solutions to Giles' objective functional: dash–dot lines, ψ_1; dashed lines ψ_2; solid lines ψ_3. Right, eq. (28): solid line, $(\partial\Psi/\partial x)^T.(S\mathbf{F})$; dashed line, pressure distribution $g(\mathbf{V}) = P$.

At a first glance, figs. 3–left and 5–left show both solutions share similar features, such as the throat singularity at the same position— although the ψ_i signs have changed. However, a closer look at them reveals the solutions behave differently through the shock wave— which is in the same position for both. In the latter case (fig. 5–left) the ψ_i cross the shock wave smoothly with zero slope, as opposed to the non–zero angles that appear in former.

As expected, the results on fig. 5–left corroborate the findings that are presented in ([Giles and Pierce, 2001]) for the same objective functional (26). The assertion becomes clearer on fig. 5, right. There it can be seen the Ψ derivatives are continuous, and reach zero at the shock wave location (solid line). Whereas the objective functional integrand $g(\mathbf{V})$ undergoes a finite jump at that point (dashed line). It is quite a different picture from fig. 4, right, where both the Ψ derivatives and $g(\mathbf{V})$ experience jumps of the same magnitude, within the results accuracy. These findings, in turn, seem to confirm the analysis of eq. (17), which relates the nature of the objective functional to the behavior of the adjoint variables through a shock wave.

5. CONCLUSIONS

The present work primary objective has been to explore the conceptual foundations of the adjoint method. Two main aspects of the topic have deserved special attention, namely: the relation between the primal and dual problems and the

well–posedness of the latter. In particular, with respect to internal conditions, the idea was to address a question that is still subject to debate in the literature.

A novel approach to the problem has been proposed, which is geared toward achieving those specific purposes. It consists in seeing the adjoint variables as generalized constraint forces, which impose realizability conditions on flow–physics variations. Within that framework, the terms that give rise to boundary conditions amount to inner products, which only vanish when the adjoint variables are orthogonal to all allowable variations— the latter are viewed as virtual displacements in the system state–space. In principle, this rationale ensures that the adjoint problem should always be well–posed. Moreover, further research into the topic seems to indicate it can be extended to a more general context. That would involve 2 and 3–D applications, besides more complex flow–physics models.

As for the internal condition, the need for imposing the adjoint variables continuity through shock wave is verified. That result certainly confirms Giles and Pierce's assertions on the subject. However, our findings also make it clear that the adjoint solution behavior through the shock location depends on the nature of the objective functional. Furthermore, they show the strength of the adjoint gradient discontinuity at that position is governed by a term that is strongly related to the non–homogeneous term of the adjoint equation. For a specific class of objective functionals, the adjoint solution remains continuous up to the first derivative at that position.

Only a few test results have been included in the paper. Nonetheless, they should suffice to support the approach that has been proposed here.

6. ACKNOWLEDGMENTS

The second author would like to acknowledge the support of FAPESP grants 97/01229-7 and 99/03105-9 which were pivotal in the development of this research paper.

7. REFERENCES

Giles, M. B. and Pierce, N. A., 1997, Adjoint Equations in CFD: Duality, Boundary Conditions and Solution Behavior, AIAA Paper 97–1850.

Giles, M. B. and Pierce, N. A., 1998, On the Properties of the Adjoint Euler Equations, Baines, M. J., editor, "Numerical Methods for Fluid Dynamics VI".

Giles, M. B. and Pierce, N. A., 1999, Adjoint recovery of superconvergent functionals from approximate solutions of partial differential equations, Report 98/18, Oxford University Computing Laboratory, Oxford.

Giles, M. B. and Pierce, N. A., 2000, Analytic Adjoint Solutions for the Quasi–1D Euler Equations, Report 00/03, Oxford University Computing Laboratory, Oxford.

Giles, M. B. and Pierce, N. A., 2001, Analytic Adjoint Solutions for the Quasi–1D Euler Equations, "Journal of Fluid Mechanics", Vol. 426, pp. 327–345.

Hirsch, C., 1994a, "Numerical Computation of Internal and External Flows", Vol. I of "Wiley Series in Numerical Methods in Engineering", John Wiley & Sons, NY, 1st edition, Fundamentals of Numerical Discretization.

Hirsch, C., 1994b, "Numerical Computation of Internal and External Flows", Vol. II of "Wiley Series in Numerical Methods in Engineering", John Wiley & Sons, NY, 1st edition, Computational Methods for Inviscid and Viscous Flows.

Jameson, A., 1988, Aerodynamic Design Via Control Theory, "12th IMACS World Congress on Scientific Computation", MAE Report 1824, Paris.

Lax, P. D., 1973, "Hyperbolic Systems of Conservation Laws and the Mathematical Theory of Shock Waves", Society for Industrial and Applied Mathematics – SIAM, Philadelphia, PA, 1st edition.

Leveque, R. J., 2002, "Finite Volume Methods for Hyperbolic Systems", Cambridge Texts in Applied Mathematics, Cambridge University Press, Boston, MA, 1st edition.

Pulliam, T. H., 1986, Artificial Dissipation Models for the Euler Equations, "AIAA Journal", Vol. 24, No. 12, pp. 1931–1940.

Vanderplaats, G. N., 1984, "Numerical Optimization Techniques for Engineering Design: With Applications", Series in Mechanical Engineering, McGraw-Hill, N.Y., 1st edition.

Volpe, E. V. and Santos, L. C. C., 2007, Boundary and Internal Conditions for Adjoint Fluid Flow Problems – Applications to Quasi–1D Euler Equations, Paper submitted to the Theoretical and Computational Fluid Dynamics Journal.

8. Responsibility notice

The authors are the only responsible for the printed material included in this paper